THE VARIATION OF STORAGE AND HEAT ENERGY IN AISI 304 UNDER PLASTIC DEFORMATION

by

Alexey LUNEV [*] ***and Mikhail NADEZHKIN***

Institute of Strength Physics and Materials Science,
Siberian Branch, Russian Academy of Sciences, Tomsk, Russia

Original scientific paper
https://doi.org/10.2298/TSCI19S2545L

The results of the analysis of heat and stored energy variation in stainless steel AISI 304 under tension are presented in this work. The distributions of temperature and strain on the surface of specimens have been obtained by using infrared thermography and the digital image correlation of laser speckle patterns techniques. It has been found that the plastic flow diagram consists of two linear stages. The first one is characterized by the monotonic growth in evolved heat. At the second linear stage the portion of stored energy rises, that is connected with the growth in the rate of martensitic transformations. A temperature fluctuation in the center of a specimen at the true strain over 0.4 appears due to the motion of localized strain bands, which are also the sources of heat.

Key words: *infrared thermography, stored energy, dissipated energy, digital image correlation, stainless steel, plastic deformation, martensitic transformation*

Introduction

Infrared thermography (IRT) is used for the transformation process investigation of applied mechanical energy in solid materials under deformation. Such investigations allow determining an energy part converted into heat as well as estimating stored energy through the rearrangement of crystal structure. In a number of papers [1-4] the studies of evolved heat variation relative to plastic deformation energy was subjected. Dissipated energy in shape-memory alloys Cu–Zn–Al, Ni–Ti, Cu–Al–Be, Ti-4.2Al-1.6Mn was studied under cyclic loading [5-8]. The investigations of materials deforming with serrated flow appearance accompanied by the nucleation of Portevin-Le Chatelier bands are subjected in several works [6, 9–11]. The analysis of temperature and strain fields obtained by IRT and the digital image correlation (DIC) of speckle patterns allows subjecting the dissipated energy in the bands with high precision.

The results of temperature measurement are also useful for the development of plastic deformation models taking into account the mechanisms of structure transformations. For example, Oliferuk *et al*. [4] and Oliferuk and Raniecki [12] performed the analysis of evolved heat variation during plastic deformation and developed corresponding constitutive model. In works [13, 14] IRT was used for thermal analysis in polymers being under deformation. Polymers have small thermal conductivity and strong dependence of temperature. These features lead to nonlinear dependence of specimen maximal temperature via loading rate during tensile tests.

[*] Corresponding author, e-mail: agl@ispms.ru

Despite the increasing number of papers in the area of the thermal investigation of plastic deformation, the change in evolved heat energy at the transition between plastic flow stages has not yet been investigated. It is known that the elastic deformation of materials is accompanied by decreasing of temperature. While at the yield limit, the dependence of temperature on strain varies from decreasing to increasing. Prefracture stage is accompanied by the growth in the dissipated heat, which is located in neck formation area. In some materials the plastic hardening curve can be split into more than one stages described as $S(e) = S_0 + Ke^n$ [15], where S is true stress, S_0 – the initial stress for given stage, e – the true strain, K – the strain hardening coefficient, and n – the hardening exponent. Stage changing can be the result of microstructure evolution during plastic deformation as well as the activation of additional mechanisms of plastic deformation (twinning, phase transformations, grain boundary sliding or grain rotation). In this case, the dependence of dissipated energy can change non-monotonically. The possibility to detect the stage changing during deformation has both fundamental and applied significance, in particular at the control of metal forming by plastic deformation.

In the presented work the variation in storage and dissipated energy at the transition area from first linear hardening stage to second one in austenitic stainless steel AISI 304 is under consideration.

Experimental procedure

The stainless steel AISI 304 specimens with the working area size 50 mm × 10 mm × 2 mm were cut from cold rolled sheet. Before loading, the specimens were quenched from 1050 ºC and then annealed at the temperature of 650 ºC during 3 hours. The specimens were loaded by uniaxial tension at a constant velocity $1.7 \cdot 10^{-4}$ s^{-1} on a universal test machine LFM-125.

Simultaneously with loading, the laser speckle patterns were recorded on one side of the specimen by high-resolution digital camera. On the opposite side of the specimen the temperature distribution was measured. A scheme of the experimental set-up is presented in fig.1. Small thickness of investigated specimen allows comparing data obtained by two techniques simultaneously. It is possible because of loading involves whole volume and can be studied on opposite side.

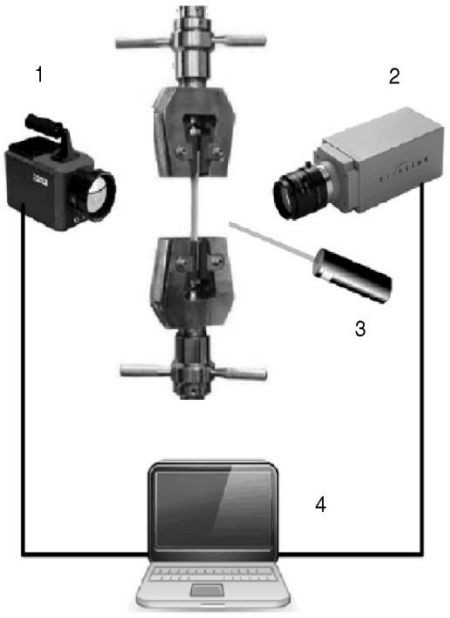

Figure 1. Experimental scheme;
1 – thermal imaging camera Flir SC7000,
2 – high-resolution digital camera,
3 – semiconductor laser, 4 – computer

The IRT was subjected with universal thermal imaging camera Flir SC7000 (1), having record rate of 5 Hz and spatial resolution of 15 μm. The treatment of obtained temperature images was performed by ALTAIR software. The distribution of temperature along a specimen (profile) was obtained in the central point of working area. Due to provide maximal surface emissivity the specimens was covered by a thin layer of black paint. The layer kept undamaged during loading test until specimen break (failure).

The environment temperature was equal 22 ºC and did not change during loading experiments.

Speckle patterns were recorded with ALMEC-tv equipment, which consists of high-resolution digital camera (2), semiconductor laser (3) and high-performance personal computer. Speckle pattern treatment was performed by DIC method. Using this method the distribution of displacement vectors $\vec{r}(x,y)$ on a specimen surface was obtained. Numerical differentiation of longitudinal u and transverse v displacement components provided data about local strains in the distortion tensor form. For plane deformation the tensor is written:

$$\beta_{ij} = \begin{vmatrix} \varepsilon_{xx} & \varepsilon_{xy} \\ \varepsilon_{yx} & \varepsilon_{yy} \end{vmatrix} + \omega_z \tag{1}$$

where $\varepsilon_{xx} = \partial u/\partial x$, $\varepsilon_{yy} = \partial v/\partial x$, $\varepsilon_{xy} = \varepsilon_{yx} = 1/2(\partial u/\partial y + \partial v/\partial x)$, and $\omega_z = 1/2(\partial v/\partial x - \partial u/\partial y)$. Due to uniaxial loading we analyzed only ε_{xx} component of the distortion tensor. An example of resulting distribution of displacement vector and ε_{xx} is shown in fig. 2.

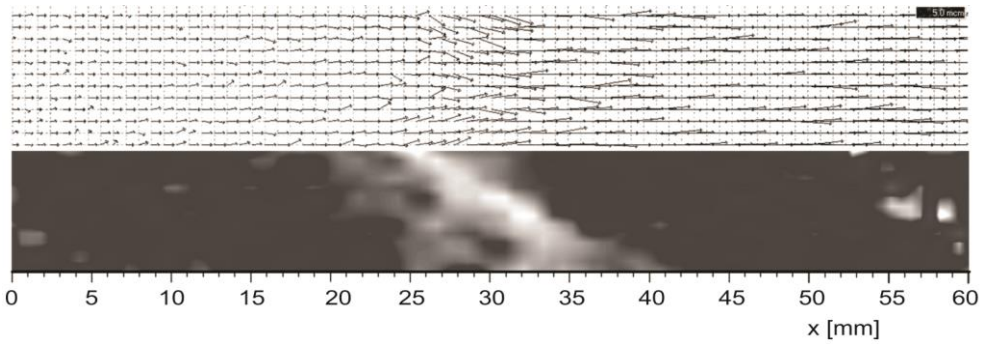

Figure 2. Distribution of displacement vectors and ε_{xx}

Energy calculation procedure

According to thermodynamic principles [17], for a specimen in the proces of deformation, incremental applied work, ΔA, transforms in stored (internal) energy, ΔW_i, of the specimen and evolution of heat, ΔQ. The change in stored energy is written:

$$\Delta W_i = \Delta A - \Delta Q \tag{2}$$

At uniaxial tension of a flat specimen, work of deformation is determined from force – elongation curve by the following equation $\Delta A = F\Delta l$, where F is the currently applied force, Δl – the elongation. In the case of constant loading rate, the elongation during preset time interval is constant as well.

Using temperature data obtained by IRT, heat dissipation energy can be calculated from heat equation:

$$\frac{\partial T}{\partial t} = \alpha\left(\frac{\partial^2 T}{\partial x^2} + \frac{\partial^2 T}{\partial y^2} + \frac{\partial^2 T}{\partial z^2}\right) + \frac{q_V}{c\rho} \tag{3}$$

where $\alpha = \lambda/c\rho$ is the thermal diffusivity, T – the measured temperature, t – the time, x,y,z – the co-ordinates along the length, the wide and depth of a specimen, respectively, λ – the thermal conductivity, c – the specific heat capacity, ρ – the density, and q_V – the volumetric heat energy generated per unit time. We assume in our experiment, that a,l,r,c are independent on co-ordinates and time.

In the current experimental condition, the main part of heat transfers from a specimen to massive grips through the contact area. It is clearly seen from the temperature distribution along the specimen length in fig. 3. Therefore, we assume that temperature along *y*- and *z-axes* remains constant, that is $\partial^2T/\partial y^2 = \partial^2T/\partial z^2 = 0$. Then eq. (3) can be solved for q_V:

$$q_V = c\rho\left(\frac{\mathrm{d}T}{\mathrm{d}t} - \alpha\frac{\partial^2 T}{\partial x^2}\right) \tag{4}$$

We let time interval 1 second for the calculation of all the deviations and assume that the heat generated in the specimen as the result of plastic deformation distributes in specimen's volume uniformly, *i. e.* notable localization of deformation does not appear. Hence, we can write that $\Delta Q = q_V V$, where V is the specimen volume keeping constant during plastic deformation. The final form of the eq. (2) can be written:

$$\Delta W_i = F\Delta l - c\rho V\left(\frac{\mathrm{d}T}{\mathrm{d}t} - \alpha\frac{\partial^2 T}{\partial x^2}\right) \tag{5}$$

Each value ΔW_i we calculated at certain strains by using eq. (5). The values $\partial^2T/\partial x^2$ were obtained from *T(x)* curve approximation by a quadratic polynomial. An example of *T(x)* approximation is shown in fig. 3. It should be noted that stored energy is the sum of elastic (reversible) and inelastic energy. We do not consider the change in elastic energy because its value per one second is equal to 10^{-7}-10^{-8} of inelastic energy.

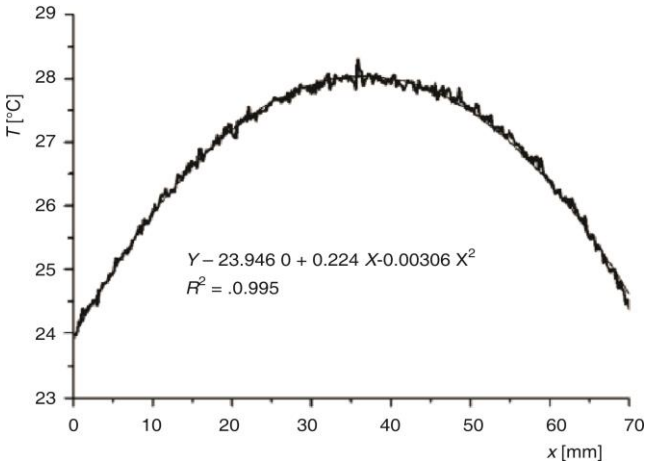

Figure 3. Temperature distribution along *x* co-ordinate and its approximation by quadratic polynomial

Results and discussion

As a result of experiments on AISI 304 steel specimens, the stress – strain diagrams and temperature distributions on specimen surface were obtained. The stages of plastic flow curves were estimated by the Ludwik equation $S(e) = S_0 + Ke^n$, where $S = \sigma(1 + \varepsilon)$, $e = \ln(1 + \varepsilon)$ σ and ε are engineering stress and strain, S_0 – the true yield stress, K – the hardening coefficient, and n – the hardening exponent. Two linear stages of the plastic flow and the transition region between them were found. In fig. 4, the true strain ranges for the linear stages is marked by Roman numerals I and II. The parameters of the linear stages are presented in tab. 1.

Table 1. The parameters of the linear stages of strain hardening

Stage	*e*	*K* [GPa]	*n*
1	0.05-0.25	1.5	1.0
2	0.32-0.58	2.1	1.0

The dependence of specimen surface temperature on true strain was drawn for the central point of the specimen at a distance of 35 mm from the stationary grip. On the temperature – true strain curve (see fig. 4) more than one characteristic regions were distinguished. Small decrease in temperature during the elastic deformation occurs due to the thermoelastic effect. Plastic deformation at the first linear stage is accompanied by monotonic increase in the tempera-

ture, caused by partial dissipation of the deformation energy into heat. At the transition region between linear stages, the temperature remained almost constant. At the second linear stage, the temperature continued to rise up to the true strain $e \approx 0.4$. Further temperature fluctuations appeared due to the motion of localized strain bands. The localization of deformation is caused by strain-induced martensitic transformations [18]. Strain bands (Portevin-Le Chatelier bands) are localized heat sources moving along the specimen. This motion leads to temperature fluctuations in the measurement point having constant position on specimen's surface. In this strain region, the assumption of the uniform distribution of heat sources in specimen volume is not valid.

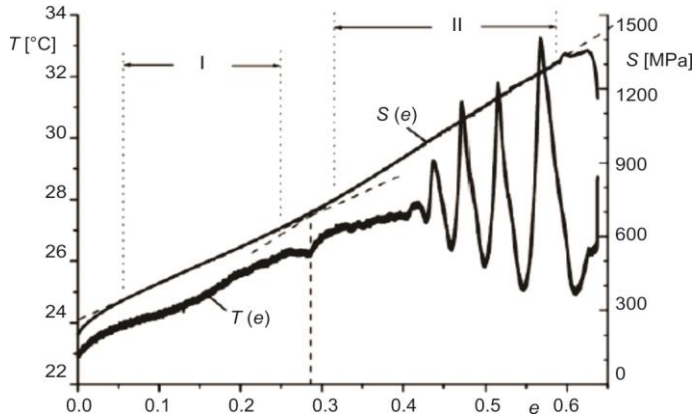

Figure 4. The dependencies of temperature and true stress on true strain in AISI 304 during tension

The analysis of the strain distribution and detection of localized strain bands was performed on the recorded speckle patterns of a specimen surface using the DIC method. The research of strain distribution was carried out at the longitudinal component of distortion tensor. It was found that the strain distributes almost uniformly up to true strain $e \approx 0.4$, after which the deformation localized in the moving along the specimen bands. In this case, the maximum value of the heat emission (maximum temperature) located in the bands. Figure 5 shows the comparison of measured longitudinal strain and temperature on the surface of the investigated specimen at true strain values 0.27, 0.47, 0.50.

The similar research of the variation of maximum temperature in AISI 304 specimens during tension at a rate of 10^{-2} s^{-1} was subjected in [19]. The authors had obtained a monotonic changing in the maximum temperature of the specimen until necking stage. The absence of stage splitting of a stress – strain curve as well as a specific region on the temperature dependence in this work is possibly connected with the heating of the specimen during deformation over 20 degrees relatively to the initial temperature. Such heating leads to austenite stability increase, which inhibits the martensitic transformations [20].

We calculated the change in the dissipated (evolved) heat and stored energy in the specimen during deformation at true strain range of 0.02-0.40. The results of the calculation in the form of the relationship of $\Delta W_i/\Delta Q$ *vs.* true strain are presented in fig. 6. At the beginning of plastic flow (at true strain value of 0.02) the ratio of stored energy and evolved heat is close to the value of 1.0. During the deformation at the first linear hardening stage, the portion of evolved heat energy was rising and had reached the value close to 100% of the applied plastic deformation work at the end of the first linear stage ($e \approx 0.25$).

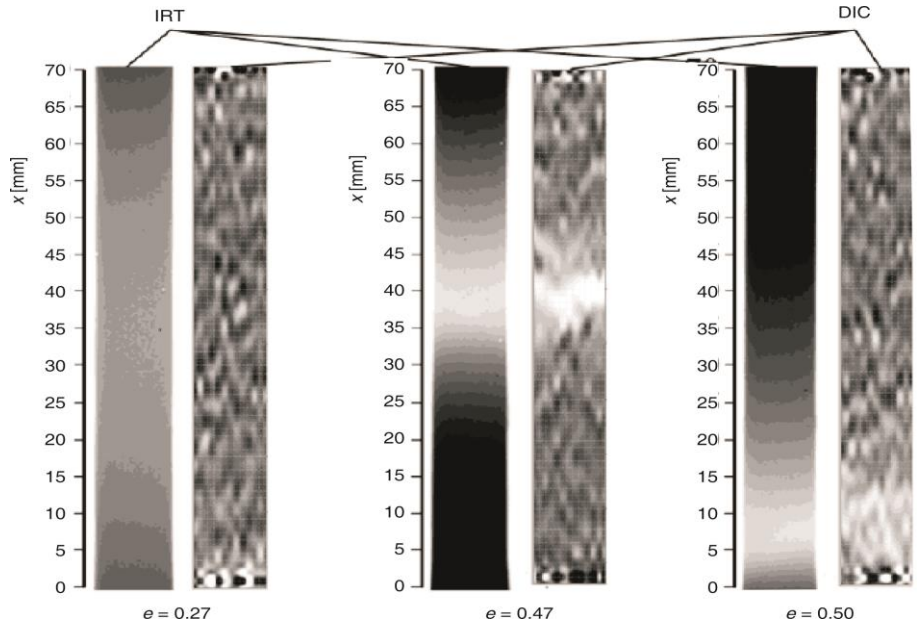

Figure 5. Temperature and elongation strain distribution on the surface of the specimen

In a region of the transition from the first linear stage to the second one (e = 0.25-0.3), the stored energy temporary increased and reached up to 15% of the applied plastic deformation work. The deformation of the specimens at the second linear stage before the localization of deformation appearance was accompanied by growth in $\Delta W_i/\Delta Q$ ratio.

The growth of stored energy at the second linear stage is associated with an increase in the rate of strain-induced martensitic transformation. According to the works [19-21], the first linear stage of hardening is connected with the deformation of austenite in AISI 304 steel and slow increase in the volume fraction of martensite. Martensite nucleates mainly near the slip bands and its distribution in the bulk of the specimen is random. At the end of the first linear stage, the volume fraction of α' martensite is about 10%. In this case, martensite forms a block structure [21], which has higher strain-hardening coefficient than that in austenite. The second linear stage is characterized by strain hardening of martensite. Simultaneously, the rate of martensitic transformation is rising. This condition, obviously, determines the growth of the stored energy relative to evolved heat energy.

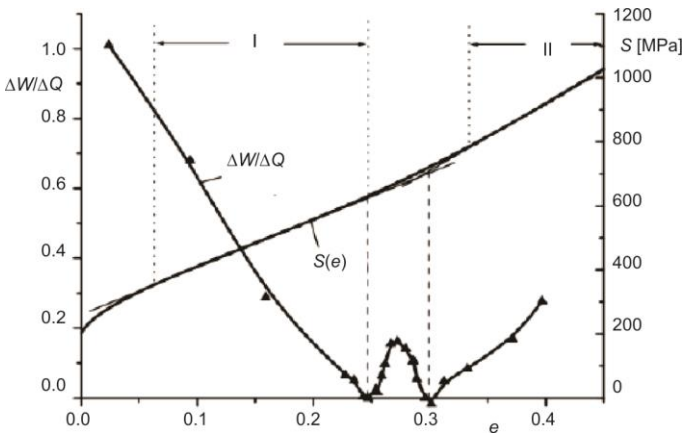

Figure 6. Stored energy relative to dissipated energy and true stress *vs.* true strain in AISI 304 during tension

Conclusions

In the result of the study of temperature and strain change in stainless steel AISI 304 under tension, it was determined the following:

- The specimens deform almost uniform before true strain $e \approx 0.4$. Further deformation proceeds with localization phenomenon appearance. Strain localizes in the moving along the specimen bands.
- Plastic flow diagram consists of two linear stages and final necking stage. During the first stage, temperature rises monotonically, whereas stored energy relative to evolved heat energy is falling. The transition between linear stages is accompanied by temperature stabilization and non-monotonic change in stored energy *vs.* evolved heat energy. At the second linear stage, before localization of deformation appearance, both the temperature and the portion of stored energy rise. This fact is elucidated by the growth in the rate of martensitic transformations.
- Temperature fluctuations in the center of the specimens at the true strain over 0.4 appear due to the motion of localized strain bands, which are also the sources of heat generation. The temperature – strain dependence becomes maximal when the band moves through a measurement point and becomes minimal when the band locates on a maximum distance from one.

Acknowledgment

The work was supported by the Russian Science Foundation (project No. 16-19-10025).

Nomenclature

ΔA – incremental applied work, [J]
c – specific heat capacity, [$\mathrm{Jkg^{-1}K^{-1}}$]
e – true strain, [–]
q_V – volumetric heat energy, [$\mathrm{Jm^{-3}s^{-1}}$]
ΔQ – evolved heat change, [J]
S – true stress, [MPa]
T – temperature, [K]
t – time, [s]
ΔW_i – stored (internal) energy change, [J]

Greek symbols

α – thermal diffusivity, [$\mathrm{m^2s^{-1}}$]
λ – thermal conductivity, [$\mathrm{Wm^{-1}K^{-1}}$]
ρ – density, [$\mathrm{kgm^{-3}}$]

References

[1] Hodowany, J., *et al*., Partition of Plastic Work into Heat and Stored Energy in Metals, *Exp. Mech.*, *40* (2000), 2, pp. 113-123
[2] Fedorova, A. Y., *et al*., Heat Dissipation Energy Under Fatigue Based on Infrared Data Processing, *Quant. InfraRed Thermogr. J.*, *11* (2014), 1, pp. 2-9
[3] Kostina, A., *et al*., Energy Dissipation and Storage in Iron Under Plastic Deformation (Experimental Study and Numerical Simulation), *Frat. Ed Integrita Strutt.*, *8* (2014), 27, pp. 28-37
[4] Oliferuk, W., *et al*., Experimental Analysis of Energy Storage Rate Components During Tensile Deformation of Polycrystals, *Mater. Sci. Eng. A*, *374* (2004), 1, pp. 77-81
[5] Bubulinca, C., *et al*., Characterization of the Mechanical Dissipation in Shape-Memory Alloys During Stress-Induced Phase Transformation, *J. Mater. Sci.*, *49* (2014), 2, pp. 701-709
[6] Muracciole, J.-M., *et al*., Energy Balance of a Semicrystalline Polymer During Local Plastic Deformation, *Strain*, *44* (2008), 6, pp. 468-474
[7] Louche, H., *et al*., Heat Source Processing for Localized Deformation with Non-Constant Thermal Conductivity. Application to Superelastic Tensile Tests of NiTi Shape Memory Alloys, *Exp. Mech.*, *52* (2012), 9, pp. 1313-1328
[8] Delpueyo, D., *et al*., Applying Infrared Thermography to Analyse Martensitic Microstructures in a Cu–Al–Be Shape-Memory Alloy Subjected to a Cyclic Loading, *Mater. Sci. Eng. A*, *528* (2011), 28, pp. 8249-8258

[9] Chrysochoos, A., *et al*., Energy Balance of Thermoelastic Martensite Transformation Under Stress, *Nucl. Eng. Des.*, *162* (1996), 1, pp. 1-12
[10] Louche, H., Chrysochoos, A., Thermal and Dissipative Effects Accompanying Lüders Band Propagation, *Mater. Sci. Eng. A*, *307* (2001), 1, pp. 15-22
[11] Wang, X. G., *et al*., Kinematic and Thermal Characteristics of Lüders and Portevin-Le Châtelier Bands in a Medium Mn Transformation-Induced Plasticity Steel, *Acta Mater.*, *124* (2017), pp. 17-29
[12] Oliferuk, W., Raniecki, B., Thermodynamic Description of the Plastic Work Partition into Stored Energy and Heat During Deformation of Polycrystalline Materials, *Eur. J. Mech. - ASolids*, *71* (2018), Sept.,-Oct., pp. 326-334
[13] Constantin, M. A., V, L. J., Temperature and Heat Effects on Polyethylene Behaviour in the Presence of Imperfections, *Thermal Science*, *20* (2016), 5, pp. 1703-1712
[14] Sedmak, S. A., *et al*., Numerical Simulation of Tensile Testing of PE 80 Polymer Specimens, *Therma Science*, *22* (2018), 1, pp. 641-649
[15] Hollomon, J. H., Tensile Deformation, *Trans. Metall. Soc. AIME*, *1945* (1945), 162, pp. 268-290
[16] Zuev, L. B., Barannikova, S. A., Experimental Study of Plastic Flow Macro-Scale Localization Process: Pattern, Propagation Rate, Dispersion, *Int. J. Mech. Sci.*, *88* (2014), Nov., pp. 1-7
[17] Prigogine, I., *Introduction to Thermodynamics of Irreversible Processes*, John Wiley and Sons Ltd, New York, USA, 1968
[18] Naraghi, R., *et al*., Spontaneous and Deformation-Induced Martensite in Austenitic Stainless Steels with Different Stability, *Steel Res. Int.*, *82* (2011), 4, pp. 337-345
[19] Rodriguez-Martinez, J. A., *et al*., Experimental Study on the Martensitic Transformation in AISI 304 Steel Sheets Subjected to Tension Under Wide Ranges of Strain Rate at Room Temperature, *Mater. Sci. Eng. A*, *528* (2011), 18, pp. 5974-5982
[20] Lichtenfeld, J. A., *et al*., Effect of Strain Rate on Stress-Strain Behavior of Alloy 309 and 304L Austenitic Stainless Steel, *Metall. Mater. Trans. A*, *37* (2006), 1, pp. 147-161
[21] Murr, L. E., *et al*., Effects of Strain State and Strain Rate on Deformation-Induced Transformation in 304 Stainless Steel: Part II. Microstructural Study, *Metall. Trans. A*, *13* (1982), 4, pp. 627-635

Paper submitted: October 1, 2018
Paper revised: November 8, 2018
Paper accepted: November 23, 2018